LETTERS

Atom-by-atom substitution of Mn in GaAs and visualization of their hole-mediated interactions

Dale Kitchen[1,2], Anthony Richardella[1,2], Jian-Ming Tang[3], Michael E. Flatté[3] & Ali Yazdani[1]

The discovery of ferromagnetism in Mn-doped GaAs[1] has ignited interest in the development of semiconductor technologies based on electron spin and has led to several proof-of-concept spintronic devices[2–4]. A major hurdle for realistic applications of $Ga_{1-x}Mn_xAs$, or other dilute magnetic semiconductors, remains that their ferromagnetic transition temperature is below room temperature. Enhancing ferromagnetism in semiconductors requires us to understand the mechanisms for interaction between magnetic dopants, such as Mn, and identify the circumstances in which ferromagnetic interactions are maximized[5]. Here we describe an atom-by-atom substitution technique using a scanning tunnelling microscope (STM) and apply it to perform a controlled study at the atomic scale of the interactions between isolated Mn acceptors, which are mediated by holes in GaAs. High-resolution STM measurements are used to visualize the GaAs electronic states that participate in the Mn–Mn interaction and to quantify the interaction strengths as a function of relative position and orientation. Our experimental findings, which can be explained using tight-binding model calculations, reveal a strong dependence of ferromagnetic interaction on crystallographic orientation. This anisotropic interaction can potentially be exploited by growing oriented $Ga_{1-x}Mn_xAs$ structures to enhance the ferromagnetic transition temperature beyond that achieved in randomly doped samples.

In $Ga_{1-x}Mn_xAs$, substituted Mn atoms at Ga sites act as acceptors donating holes that are believed to be responsible for mediating ferromagnetic interactions between Mn *d*-orbital core spins. Mean-field theories based on this scenario have captured the increase of the ferromagnetic transition temperature, T_c, with doping and other macroscopic properties of $Ga_{1-x}Mn_xAs$ (refs 5, 6). Experimental efforts have also shown that improved material quality, achieved through various methods including annealing of random alloy samples, can significantly increase T_c even above 150 K (refs 7–10). However, we lack an accurate microscopic picture that will identify the precise nature of hole states involved and provide clues on how to enhance ferromagnetism in this compound. Previous STM experiments have mapped the shape of single acceptor states for Mn in subsurface sites[11], but have been unable to observe interactions between them directly[12]. First-principles calculations[13,14] have provided insight, but their predictions for the structure of Mn–Mn interactions could only be tested statistically in macroscopic materials that also contained large numbers of defects, interstitials and other complicating features.

We performed our experiments using a home-built cryogenic STM that operates at 4 K in ultrahigh vacuum. We used wafers of GaAs doped with 10^{18}–10^{19} Zn atoms cm^{-3}, which are cleaved *in situ* to expose a (110) surface. The cleaved samples show STM topography and spectroscopy that are characteristic of a degenerately doped p-type GaAs sample, with the Fermi level very close to the valence band edge of the GaAs[15]. Although the (110) surface undergoes a small reconstruction, there are no surface states at energies within the GaAs gap to complicate our studies[16]. To substitute Mn atoms for Ga, we first deposited a small concentration of Mn atoms (0.1–2% monolayer) from an *in situ* source onto the cold sample surface. The deposited Mn atoms are weakly adsorbed on the surface, appearing in valence-band images (tip-sample bias $V < 0$) of a GaAs (110) surface as small protrusions (Fig. 1a and b) and can be manipulated using the STM tip.

We discovered that application of a voltage pulse in the STM junction, which injects energetic electrons onto a Mn adsorbate's site, results in the substitution of one Mn for one Ga atom in the surface layer. This substitution process requires us to inject electrons with energies of 0.7 eV or higher. Varying the precise placement of the tip near the adsorbate resulted in either its substitution or its lateral motion on the surface. Figure 1c and d, after tip-voltage pulses, reveal the presence of the substituted Mn by showing its influence on neighbouring As atoms and the ejection of the Ga atom it has replaced. The precise physical process for the STM-assisted substitution is still under investigation; nonetheless, model calculations show that the substituted configuration of Mn has a lower energy than the adsorbate configuration on the GaAs (110) surface[17]. We found that the STM-assisted incorporation and motion of Mn adsorbates can be used to substitute Mn atoms successfully at precise

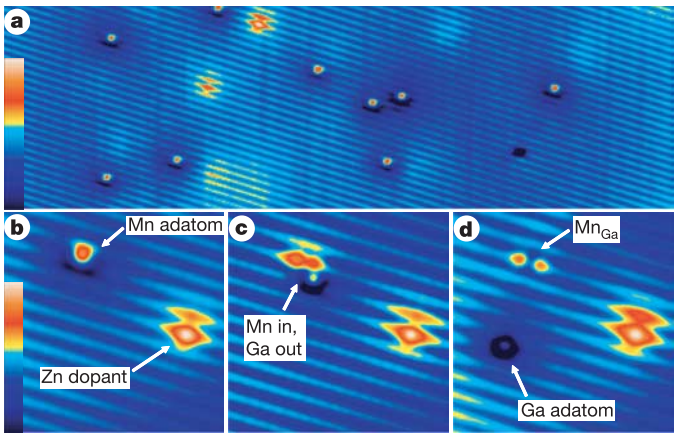

Figure 1 | Single-atom substitution of one Mn for one Ga atom. a, Large topograph of the occupied states (500×150 Å^2; -2 V; 0–1.5 Å) showing many Mn adsorbates and a few subsurface Zn dopants. **b–d**, High-resolution topographs (75 Å^2; -2 V; 0–1.3 Å). **b**, Mn adsorbate and a Zn acceptor visible on the As sublattice. **c**, STM-assisted incorporation of the Mn into a Ga site forcing the substituted Ga atom to the surface. **d**, Tip-pulses move the Ga adatom from the incorporation site, isolating a Mn acceptor (Mn_{Ga}).

[1]Department of Physics, Joseph Henry Laboratories, Princeton University, Princeton, New Jersey 08544, USA. [2]Department of Physics, University of Illinois at Urbana-Champaign, Urbana, Illinois 61801, USA. [3]Optical Science and Technology Center and Department of Physics and Astronomy, University of Iowa, Iowa City, Iowa 52242, USA.

Ga sites and to remove the ejected Ga atoms from the substitution area. All the experimental results reported here were repeated for Mn at different locations on the surface to ensure that interaction with native Zn acceptors in the substrate did not alter our experimental findings.

The modifications of the local density of electronic states (LDOS) of GaAs due to Mn substitution significantly affect the nature of their interactions within the GaAs host. We probed these modifications by combining real space imaging together with spatially resolved STM spectroscopy, performed by measuring the differential conductance, dI/dV versus V (where I is current and V is voltage), using standard lock-in techniques. The spectroscopic measurements performed in the vicinity of an isolated substituted Mn are shown in Fig. 2a. The modification of the valence-band electronic states ($V < 0$ in the spectra), as indicated by an arrow in the tunnelling spectra of Fig. 2a, is strongest on the As neighbours nearest the Mn. The spatial extent of the Mn-induced modifications of the valence-band states is weak beyond the nearest As neighbours and is spatially anisotropic, as shown in Fig. 2b. The Mn has a greater influence, however, owing to the binding of an acceptor state to the Mn site producing a strong resonance in the tunnelling spectra inside the GaAs gap (Fig. 2a). The dominance of the Mn acceptor state in the LDOS lends itself to direct mapping of the acceptor-state wavefunction in the unoccupied state images. Such images, as shown in Fig. 2c, demonstrate that the Mn acceptor has an anisotropic star-shaped spatial structure that is distributed over more than a 20 Å^2 area of the surface[18]. The large energy width (>150 meV) of the conductance peak shows that the Mn acceptor state has a large overlap with the continuum states, such as those due to Zn acceptors, in our substrates, eliminating the possibility of charging effects when tunnelling through this state.

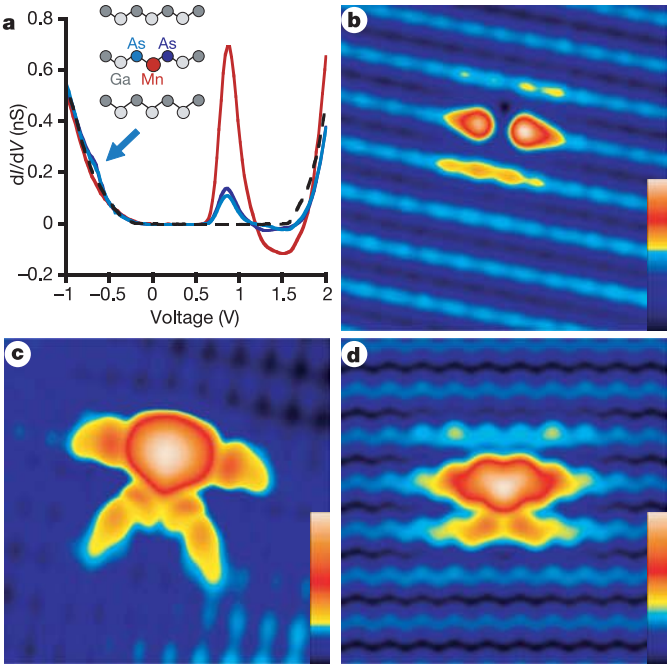

Figure 2 | High-resolution measurements of a single Mn acceptor (Mn_{Ga}). a, Spatially resolved dI/dV measurements near an Mn acceptor. The As neighbours show enhancements deep in the valence band, highlighted by the blue arrow. The large in-gap resonance over the Mn is its acceptor level. **b**, 40 Å^2 topograph of the occupied states (−1.5 V; 0–0.4 Å) showing enhancements concentrated on the neighbouring As. **c**, 40 Å^2 topograph of the unoccupied states (+1.55 V; 0–4 Å) revealing the anisotropic shape of the Mn acceptor. **d**, Tight-binding model of a Mn acceptor in bulk GaAs with the Mn spin oriented in-plane along [001]. The image shows a 40 Å^2 area of the (110) plane containing the Mn. The log of the integrated LDOS from the Fermi level to 1.55 eV is displayed with a spatial broadening factor of 1.7 Å. The colours in the scales have been chosen to enhance the view of the Mn influence on GaAs.

The measured modifications of the LDOS, induced by Mn in the (110) surface layer of GaAs, are consistent with tight-binding calculations of the electronic states in bulk GaAs near Mn acceptors (see Supplementary Information)[19]. Figure 2d shows a simulated STM image of the acceptor state based on the bulk tight-binding calculations that model the experimental situation by showing the calculated electronic states near a Mn dopant in the bulk at the (110) layer containing the Mn. These calculations have essentially one free parameter, the p–d hybridization induced by the Mn site, which is adjusted to match the measured bulk acceptor level energy. The spatial structure of the calculated wavefunction for the bulk acceptor shows a similar anisotropic shape and extent as seen in the STM experiment for Mn at the surface. The tight-binding calculations also predict resonances deep within the valence band[19], which account for the valence-band modification imaged in Fig. 2b. These resonance states have been anticipated[19] to play a part in interpretation of photoemission[20] and infrared optical conductivity[21,22] measurements of $Ga_{1-x}Mn_xAs$.

More detailed comparisons of our measurements with the bulk calculations and with other STM measurements of subsurface Mn[11] provide ways to assess the significance of the surface in our findings. Simulating the impact of the surface on the acceptor state in the bulk calculation by adjusting the potential energy of one of the As bonded to the Mn, we find that the acceptor state shifts deeper into the gap. Our experimentally measured acceptor state is indeed found deeper in the gap (850 meV), as compared to the measured value for the bulk (113 meV), although a significant part of the observed shift is due to tip-induced band-bending typical of tunnelling between a metal and a semiconductor[15,16]. More importantly, contrasting our measurements with recent STM studies of $Ga_{1-x}Mn_xAs$ samples grown by molecular-beam epitaxy[11], the subsurface Mn acceptors show states with similar anisotropic symmetry and spatial extent to those reported here. In the studies of subsurface Mn, tunnelling through the layers of GaAs broadens some of the finer features of the acceptor state compared to that reported here—a behaviour captured by our tight-binding model (see Supplementary Information). Overall, comparison of our data to bulk calculations and to previous STM measurements of Mn in subsurface sites shows that surface effects do not significantly alter the acceptor state's characteristics. This comparison motivates the study of the interaction between STM-substituted Mn atoms as a model situation for probing the nature of Mn–Mn interactions mediated through the GaAs host.

Our atom-by-atom substitution technique provides a powerful method of implanting Mn acceptors at precise relative separations and orientations in the GaAs surface and to examine their interaction in pairs. Figure 3 details measurements of an STM-substituted Mn pair, separated by 8 Å along a <110> crystallographic direction. Figure 3a and b shows changes in topography induced in the GaAs valence band and in-gap states by the Mn pair. Direct evidence for interaction within the pair can be observed in the tunnelling spectra of Fig. 3c, which reveals splitting of the acceptor state into two resonances. Figure 3d and e shows results of conductance mapping, which probes the spatial characteristic of electronic states by visualizing changes in dI/dV at specific energies, confirming that the split states observed in the spectra (Fig. 3c) indeed have bonding/anti-bonding characteristics. In this situation, the observed bonding state occurs at higher energies because of the hole-like nature of the states involved, for which the continuum is at the top of the valence band. The observed splitting in Fig. 3 also indicates that the spin states associated with the Mn's 3d orbitals are ferromagnetically aligned. Because the formation of bonding and anti-bonding states requires electronic states that are degenerate in both energy and spin alignment, anti-ferromagnetically aligned Mn pairs would have anti-aligned acceptor states that would not show any splitting[23]. Within a doping-dependent superexchange model of magnetism (for example, ref. 24),

this state splitting is the dominant contribution to the Mn–Mn spin interaction.

Constructing Mn pairs using our atom-by-atom substitution technique and measuring the energy splitting of their acceptor states provides a method of mapping the relative strength of Mn–Mn interactions as a function of distance and crystallographic orientation in GaAs. A subset of the Mn pairs we have examined is shown in Fig. 4a–d and Fig. 3b, along with measurements of the splitting energy of the acceptor levels for Mn pair configurations up to the six nearest neighbours in Fig. 4e. Our key observation is that the Mn–Mn interaction decays rapidly with increasing separation between the Mn acceptors and is highly anisotropic. The data in Fig. 4e clearly show that pairs constructed along <110> crystallographic directions have a much stronger splitting than those along the <100> or <111> directions. Our ability to probe the energy splitting of the pairs is limited by the energy width of a single Mn acceptor state. Consequently, based on experimental measurements alone, we cannot rule out the possibility that pairs, such as the one separated by 5.65 Å along a <100> direction, that do not show splitting are not anti-ferromagnetically aligned (see Supplementary Information). Nonetheless, the experimental measurements of the relative strength of the Mn–Mn interactions and their anisotropic character can be used as a test bed for microscopic models of ferromagnetic interactions in GaAs.

As a starting point for understanding our experimental findings for Mn pairs, we turn again to bulk tight-binding calculations, which successfully accounted for the Mn-induced changes in the LDOS of GaAs (Fig. 2d). We calculate splitting of the acceptor states for two bulk Mn atoms at the five nearest-neighbour pairs probed in the STM experiments, assuming that their core spins are ferromagnetically aligned and point along a <100> direction, the bulk easy axis. As shown in Fig. 4e, the results of these tight-binding calculations agree remarkably well in the overall trend and the observed anisotropy of the experimental data. The discrepancy in the actual values of acceptor-level energy splitting is probably a result of the non-trivial shift of these levels due to tip-induced band-bending in the experiment. The tight-binding model can also be used to estimate the energy gained for ferromagnetic alignment and its connection to the acceptor-state energy splitting (see Supplementary Information).

Looking beyond the tight-binding model, first-principles *ab initio* calculations also predict the same anisotropy in ferromagnetic interactions[24] that we find in our STM measurements of the state splittings for the first several nearest-neighbour pairs. In fact, various theoretical models that include detailed band structure of GaAs or the effects of spin-orbit coupling predict anisotropic Mn–Mn interactions of various degrees[25,26]. Detailed examination of our experimental data for a single Mn shows that the origin of the anisotropic splittings is most probably the shape of the acceptor wavefunction, which favours resonant interaction along the <110> crystallographic directions. However, valence-band modification of the electronic states due to Mn has a similar anisotropy, which could also mediate anisotropic interactions with a similar symmetry. In addition, spin-orbit interactions also produce crystalline magnetic anisotropy in GaMnAs. Our tight-binding model, which can be used to estimate this anisotropy for Mn pairs, shows that their spin alignment favours the <100> direction at the surface (see Supplementary Information).

Besides providing experimental results for testing models of Mn–Mn interactions in GaAs, our experiments provide microscopic information that potentially can be used to enhance ferromagnetism in $Ga_{1-x}Mn_xAs$. The significance of the experiments is perhaps best realized by considering the separations between Mn acceptors in randomly doped $Ga_{1-x}Mn_xAs$ at concentrations required for the highest reported ferromagnetic temperatures[7–10]. At 5% doping, 98% of the Mn dopants have one or more neighbour at the sixth nearest-neighbour or closer. The experiments reported here suggest that randomly distributed Mn doping fails to take advantage of the large strength of the interaction along the <110> direction. MBE-grown heterostructures could be optimized to increase the concentration of Mn dopants with <110> neighbours, and potentially enhance ferromagnetic Mn-Mn coupling. In addition, the possibility that some of the closely spaced pairs, such as the one separated by 5.65 Å along a <100> direction, could be antiferromagnetically aligned raises the question of whether spin frustration[25] could be hampering efforts to increase the ferromagnetic transition temperature in the randomly doped system.

The atom-by-atom substitution technique we have demonstrated

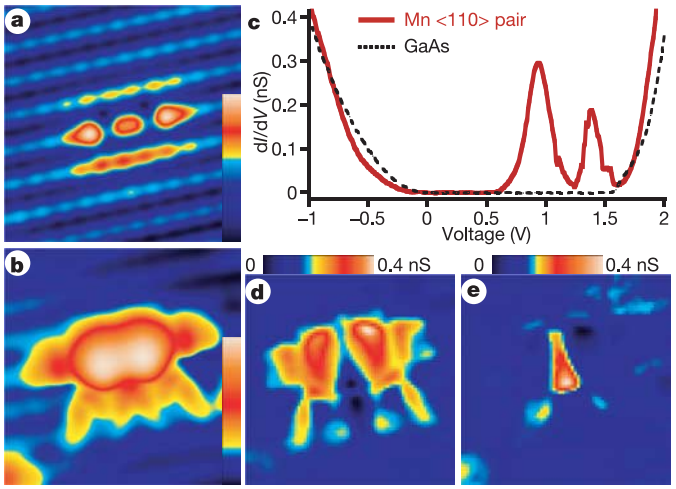

Figure 3 | Mn pair substituted in Ga sites spaced 8 Å apart in a <110> orientation. **a**, 40 Å^2 topograph of the valence-band states (−1.5 V; 0–0.4 Å). **b**, 40 Å^2 topograph of the in-gap states showing the bound states of Mn acceptors (+1.1 V; 0–4 Å). **c**, d*I*/d*V* measurements near the Mn pair, revealing two resonance levels in the gap. **d**, Differential conductance energy map at +1.35 V displaying the bonding nature of the higher energy resonance. **e**, Energy map at +0.91 V displaying the anti-bonding nature of the lower energy peak.

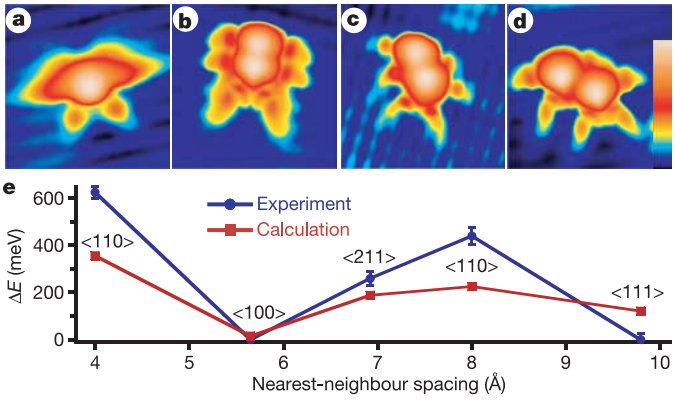

Figure 4 | Topographs (40 Å^2, +1.5 V) of several Mn pairs and the acceptor-level splitting energy of these pairs. **a**, Nearest-neighbour Mn acceptor pair (4 Å spacing, <110> orientation). **b**, Second-nearest-neighbour pair (5.65 Å spacing, <100> orientation). **c**, Third-nearest pair (6.92 Å spacing, <211> orientation). **d**, Sixth-nearest-neighbour pair (9.79 Å spacing, <111> orientation). Figure 3b shows the fourth-nearest-neighbour pair (8 Å spacing, <110> orientation). The fifth-nearest-neighbour is not accessible in a single (110) plane. **e**, Comparative plot of the Mn acceptor-level splitting for Mn–Mn pair interactions. Theory and experiment both show that Mn–Mn interactions are highly anisotropic, favouring <110> orientations. Error bars correspond to the standard deviation of many pairs measured on p-type GaAs (110) surfaces. Δ*E*, splitting energy of the acceptor levels.

here can also be an important tool in a number of new directions. A direct extension would be to use our technique to substitute other dopants in various semiconducting surfaces, as a method to search for strongly interacting ferromagnetic donors or acceptors. Such an effort can be guided by theoretical efforts similar to those described here. Single dopant substitution also provides a controlled method to create single spin quantum bits in semiconductors[27]. The tight-binding calculations show the exciting possibility that the spin-orbit coupling can dictate the shape of a single acceptor wavefunction, hence providing a method for obtaining spin information from measurements of LDOS distribution[28].

Received 3 April; accepted 6 June 2006.

1. Ohno, H. *et al.* (Ga,Mn)As: A new diluted magnetic semiconductor based on GaAs. *Appl. Phys. Lett.* **69,** 363–365 (1996).
2. Ohno, H. *et al.* Electric-field control of ferromagnetism. *Nature* **408,** 944–946 (2000).
3. Ohno, Y. *et al.* Electrical spin injection in a ferromagnetic semiconductor device heterostructure. *Nature* **402,** 790–792 (1999).
4. Eid, K. F. *et al.* Exchange biasing of the ferromagnetic semiconductor $Ga_{1-x}Mn_xAs$. *Appl. Phys. Lett.* **85,** 1556–1558 (2004).
5. Macdonald, A. H., Schiffer, P. & Samarth, N. Ferromagnetic semiconductors: moving beyond (Ga,Mn)As. *Nature Mater.* **4,** 195–202 (2005).
6. Dietl, T., Ohno, H., Matsukura, F., Cibert, J. & Ferrand, D. Zener model description of ferromagnetism in zinc-blende magnetic semiconductors. *Science* **287,** 1019–1022 (2000).
7. Edmonds, K. *et al.* High-Curie-temperature $Ga_{1-x}Mn_xAs$ obtained by resistance-monitored annealing. *Appl. Phys. Lett.* **81,** 4991–4993 (2002).
8. Ku, K. C. *et al.* Highly enhanced Curie temperature in low-temperature annealed [Ga,Mn]As epilayers. *Appl. Phys. Lett.* **82,** 2302–2304 (2003).
9. Chiba, D., Takamura, K., Matsukura, F. & Ohno, H. Effect of low-temperature annealing on (Ga,Mn)As trilayer structures. *Appl. Phys. Lett.* **82,** 3020–3022 (2003).
10. Edmonds, K. W. *et al.* Mn interstitial diffusion in (Ga, Mn)As. *Phys. Rev. Lett.* **92,** 037201 (2004).
11. Yakunin, A. M. *et al.* Spatial structure of an individual Mn acceptor in GaAs. *Phys. Rev. Lett.* **92,** 216806 (2004).
12. Yakunin, A. M. *et al.* Spatial structure of Mn-Mn acceptor pairs in GaAs. *Phys. Rev. Lett.* **95,** 256402 (2005).
13. Sanvito, S., Theurich, G. & Hill, N. A. Density functional calculations for III–V diluted ferromagnetic semiconductors: a review. *J. Supercond.* **15,** 85–104 (2002).
14. Mahadevan, P. & Zunger, A. First-principles investigation of the assumptions underlying model-Hamiltonian approaches to ferromagnetism of 3*d* impurities in III–V semiconductors. *Phys. Rev. B* **69,** 115211 (2004).
15. Feenstra, R. M. & Stroscio, J. A. Atom-selective imaging of the GaAs(110) surface. *Phys. Rev. Lett.* **58,** 1192–1195 (1987).
16. Feenstra, R. M. & Stroscio, J. A. Tunneling spectroscopy of the GaAs(110) surface. *J. Vac. Sci. Technol. B* **5,** 923–929 (1987).
17. Fu, H., Ye, L., Zhang, K. & Xie, X. Chemisorption of Mn on a GaAs(110) surface. *Surf. Sci.* **341,** 273–281 (1995).
18. Kitchen, D., Richardella, A. & Yazdani, A. Spatial structure of a single Mn impurity state on GaAs (110) Surface. *J. Supercond.* **18,** 23–28 (2005).
19. Tang, J.-M. & Flatté, M. E. Multiband tight-binding model of local magnetism in $Ga_{1-x}Mn_xAs$. *Phys. Rev. Lett.* **92,** 047201 (2004).
20. Okabayashi, J. *et al.* Angle-resolved photoemission study of $Ga_{1-x}Mn_xAs$. *Phys. Rev. B* **64,** 125304 (2001).
21. Singley, E. J., Kawakami, R., Awschalom, D. D. & Basov, D. N. Infrared probe of itinerant ferromagnetism in $Ga_{1-x}Mn_xAs$. *Phys. Rev. Lett.* **89,** 097203 (2002).
22. Burch, K. S. *et al.* Impurity band conduction in a high temperature ferromagnetic semiconductor. Preprint at ⟨http://arXiv.org/cond-mat0603851⟩ (2006).
23. Flatté, M. E. & Reynolds, D. E. Local spectrum of a superconductor as a probe of interactions between magnetic impurities. *Phys. Rev. B* **61,** 14810–14813 (2000).
24. Mahadevan, P., Zunger, A. & Sarma, D. D. Unusual directional dependence of exchange energies in GaAs diluted with Mn: Is the RKKY description relevant? *Phys. Rev. Lett.* **93,** 177201 (2004).
25. Zaránd, G. & Jankó, B. $Ga_{12x}Mn_xAs$: A frustrated ferromagnet. *Phys. Rev. Lett.* **89,** 047201 (2002).
26. Timm, C. & MacDonald, A. H. Anisotropic exchange interactions in III–V diluted magnetic semiconductors. *Phys. Rev. B* **71,** 155206 (2005).
27. Kane, B. M. A silicon-based nuclear spin quantum computer. *Nature* **393,** 133–137 (1998).
28. Tang, J.-M. & Flatté, M. E. Spin-orientation-dependent spatial structure of a magnetic acceptor state in a zinc-blende semiconductor. *Phys. Rev. B* **72,** 161315(R) (2005).

Supplementary Information is linked to the online version of the paper at www.nature.com/nature.

Acknowledgements This work was supported by the US ARO MURI and the US NSF.

Author Information Reprints and permissions information is available at npg.nature.com/reprintsandpermissions. The authors declare no competing financial interests. Correspondence and requests for materials should be addressed to A.Y. (yazdani@princeton.edu).